IL NUOVO CIMENTO **48 C** (2025) 18
DOI 10.1393/ncc/i2025-25018-1

Colloquia: WPCF-Resonance 2023

Correlations between anisotropy flow and mean transverse momentum using subevent cumulants in small systems at CMS

Rohit Kumar Singh on behalf of the CMS Collaboration
Indian Institute of Technology - Madras, Chennai, India

received 23 July 2024

Summary. — A measurement of correlations between mean transverse momentum and multiparticle cumulants in pp at $\sqrt{s} = 13$ TeV, proton-lead (pPb) at $\sqrt{s_{NN}} = 8.16$ TeV and peripheral lead-lead (PbPb) collisions at $\sqrt{s_{NN}} = 5.02$ TeV are presented for Fourier harmonics $n = 2$ and $n = 3$. Notably, sign changes in modified Pearson correlators are observed in pp and pPb systems as a function of charged particle multiplicity, but these changes disappear with increased pseudorapidity gap. Four-particle cumulants ($c_n\{4\}$) correlated with mean transverse momentum (p_T) also show no sign change, suggesting a reduced nonflow contribution. Further studies of nonflow using the color-glass condensate model is required to understand the origin of azimuthal anisotropy in small systems. Negative correlations between $c_3\{2\}$ and mean p_T are consistent across all collision systems. Comparisons with hydrodynamic predictions in pPb indicate a better fit with a smaller initial fireball.

1. – Introduction

The quark-gluon plasma (QGP), a hot and dense medium, has been extensively studied through heavy ion collisions at RHIC [1,2] and LHC [3-5]. The azimuthal anisotropy of the charged particles produced in these collisions, characterized by Fourier coefficients (v_n) in the azimuthal angle distribution $\mathrm{dN/d}\phi \propto 1 + 2\sum_n v_n \cos[\mathrm{n}(\phi - \Psi_\mathrm{n})]$, serves as a powerful tool to investigate the collective dynamics and transport properties of the QGP. The Fourier harmonics are a result of final-state response to the initial geometry of colliding system [6]. In the past decade, signatures of azimuthal anisotropy has been observed in smaller collision systems, such as proton-proton (pp), proton-lead (pPb) [7,8] similar to heavy ion collision systems like lead-lead (PbPb). This similarity exists even in the case of multiparticle correlations, which can suppress few particle correlations called 'nonflow' that has no relevance to the bulk properties of the medium [9]. In the case of small systems, the observed anisotropy can be attributed to initial-state effects, for example, as described by the color-glass condensate effective theory [10] in addition to final-state effects. The primary source of azimuthal anisotropy in small systems remains a topic of ongoing debate [11], because there has not been a definitive observable found to distinguish between initial- and final-state effects.

Besides creating the azimuthal anisotropy observed in the final state due to the initial geometric anisotropy, the hydrodynamic response to the overall size of the initial overlap area of the two colliding nuclei leads to radial flow, which adds to the mean transverse momentum ($[p_{\mathrm{T}}]$) on a event-by-event basis. The association between radial and anisotropic flow can be measured using a modified linear correlator [12],

$$\rho(v_n^2, [p_{\mathrm{T}}]) = \frac{\mathrm{cov}(v_n^2, [p_{\mathrm{T}}])}{\sqrt{\mathrm{Var}(v_n^2)_{\mathrm{dyn}}}\sqrt{\mathrm{Var}([p_{\mathrm{T}}])_{\mathrm{dyn}}}}, \tag{1}$$

where $\mathrm{cov}(v_n^2, [p_{\mathrm{T}}])$ is the covariance between v_n^2 and $[p_{\mathrm{T}}]$, and $\mathrm{Var}(v_n^2)_{\mathrm{dyn}}$ and $\mathrm{Var}([p_{\mathrm{T}}])_{\mathrm{dyn}}$ are the dynamical variances of the v_n^2 and $[p_{\mathrm{T}}]$ distributions, respectively. The dynamical variances remove the auto-correlation effects when compared with variances of v_n^2 and $[p_{\mathrm{T}}]$ distributions, and better capture the intrinsic initial-state fluctuations. This correlator is sensitive to the degree of subnucleon fluctuations, and its magnitude can be traced back to the initial density profile [13].

Recently it was suggested that this correlator could potentially differentiate between initial- and final-state effects [14]. A change in sign of the $\rho(c_n\{2\}, [p_{\mathrm{T}}])$ correlator is predicted going from high-multiplicity (dominated by final-state effects) to very low-multiplicity (dominated by initial-state effects) regions in small collision systems. However, no sign change would be present without the initial-state effects as suggested by the CGC effective theory. Studies using the PYTHIA 8 event generator with the A2 tune have showed that a sign change can exist due to nonflow effects [15]. Measurements of the correlator with proper treatment of nonflow effects, and the searches for sign changes in low-multiplicity pp, pPb, and peripheral PbPb collisions can provide insights into the origin of the azimuthal correlations in small systems. In these proceedings, the correlators are measured for the first time using four-particle cumulants instead of two-particle correlation techniques in pp, pPb, and peripheral PbPb collisions. Nonflow effects are further studied using different pseudorapdity (η) gaps. In addition, the correlators for the third Fourier harmonic are presented for the first time in the three small collision systems as a function of charged-particle multiplicity.

2. – Analysis method

Previous studies of the correlator have relied on v_n^2 extracted from two-particle correlations in eq. (1). The v_n^2 term can be expressed as the two-particle cumulant since $c_n\{2\} = \langle e^{in(\phi_1-\phi_2)}\rangle = v_n\{2\}^2$ [16]. All previous measurements have applied the subevent method to remove nonflow in the two- particle v_n [17]. With two subevents for $c_n\{2\}$, the covariance of the correlator in eq. (1) is

$$\mathrm{cov}(c_n\{2\}, [p_{\mathrm{T}}]) = \mathfrak{Re}\Big\langle \sum_{a,b} \exp^{in(\phi_a-\phi_b)}\left([p_{\mathrm{T}}] - \langle[p_{\mathrm{T}}]\rangle\right)\Big\rangle, \tag{2}$$

where ϕ_a and ϕ_b are the azimuthal angles of particles a and b in subevents A and B, respectively. The $\langle[p_{\mathrm{T}}]\rangle$ is the average $[p_{\mathrm{T}}]$ in all the events of a certain multiplicity range. Tracks with $\eta < -0.75$ are assigned subevent A, tracks with $\eta > 0.75$ assigned as subevent B and tracks in the middle region $|\eta| < 0.5$ are used to obtain $[p_\mathrm{T}]$ in each event. The selections ensure subevents A and B are symmetric in η, and that there is a minimum η gap of 1.5 between them to reduce nonflow effects. The remaining nonflow is addressed with two approaches. In the first approach, we increase the minimum η gap between subevents A and B from 1.5 to 2.0 by changing $c_2\{2\}$ calculation using particles in $|\eta| > 0.75$ to $|\eta| > 1.0$. In the second approach, we extend the current observable by replacing $c_2\{2\}$ with four-particle cumulant $c_2\{4\}$ [18]. Particles in $|\eta| > 0.75$ are divided into three equal η regions to obtain $c_2\{4\}$ in each event. The event-by-event $c_2\{4\}$ is then correlated with $[p_\mathrm{T}]$ in the same event. The results are presented as a function of tracking efficiency corrected multiplicity N_{ch} using particles within $0.5 < p_T < 5$ GeV and $|\eta| < 2.4$. Details about the CMS detector and this analysis can be found in ref. [18].

3. – Results

The measurements of covariances from two- and four-particle correlations for the second- and third-order Fourier harmonics in 13 TeV pp, 8.16 TeV pPb, and 5.02 TeV PbPb collisions are presented in fig. 1. In both pp and pPb collisions, $\mathrm{cov}(c_2\{2\}, [p_\mathrm{T}])$ for $|\eta| > 0.75$ undergoes a sign change from positive to negative as N_{ch} increases. This trend is consistent with the prediction of a sign change feature from the color-glass condensate model. However, no clear sign change is observed in pp and pPb collisions for $\mathrm{cov}(c_2\{4\}, [p_\mathrm{T}])$ and its values are consistent with 0 in pp collisions within the current statistical precision. To compare $\mathrm{cov}(c_2\{2\}, [p_\mathrm{T}])$ and $\mathrm{cov}(c_2\{4\}, [p_\mathrm{T}])$ in the same scale,

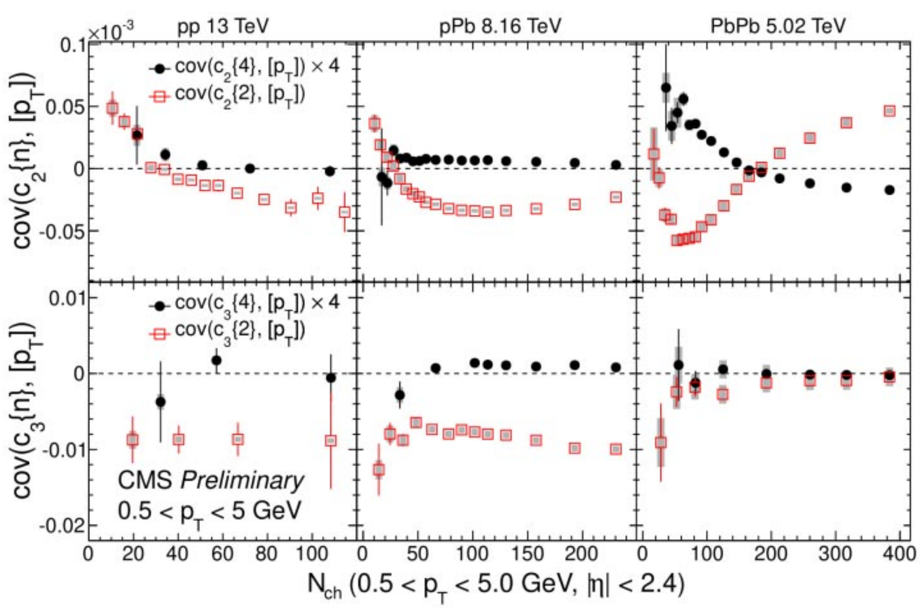

Fig. 1. – The covariances between two- and four-particle cumulant and $[p_\mathrm{T}]$ as a function of charged particle multiplicity (N_ch) in 13 TeV pp (left), 8.16 TeV pPb (middle), and 5.02 TeV PbPb (right) collisions. The two-particle cumulants are calculated with $|\eta| > 0.75$. The upper (lower) panels show the second (third) harmonics. The error bars represent statistical uncertainties, while the shaded regions indicate systematic uncertainties.

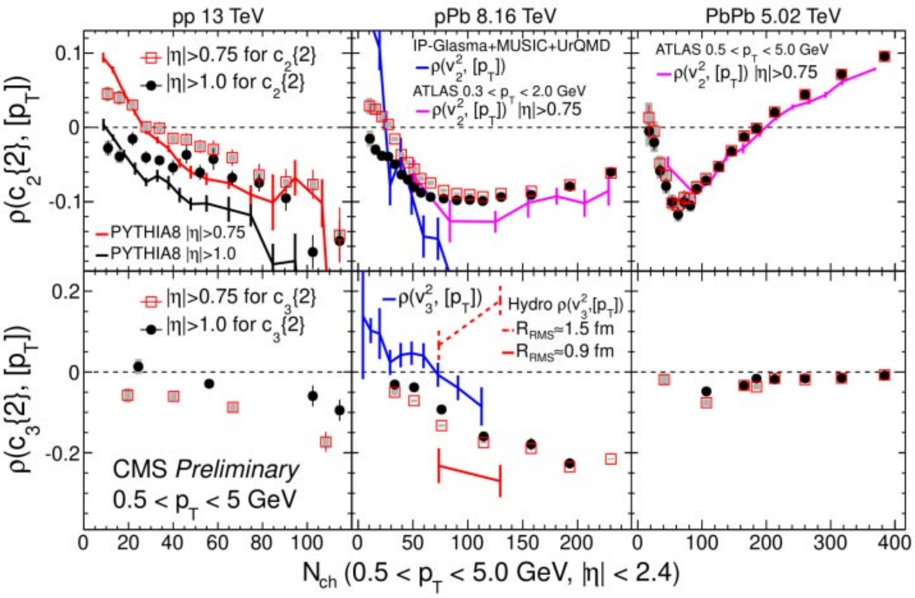

Fig. 2. – The correlator using the two-particle cumulant from $|\eta| > 0.75$ and $|\eta| > 1.0$ is presented as a function of $N_{\rm ch}$ in 13 TeV pp (left), 8.16 TeV pPb (middle), and 5.02 TeV PbPb (right) collisions. The upper (lower) panels depict the second (third) harmonics. Statistical uncertainties are represented by error bars, while shaded regions indicate systematic uncertainties. Comparisons with calculations from PYTHIA 8 (upper left panel, red and black lines) and IP-Glasma+MUSIC+UrQMD (middle panels, blue lines) [14] are provided alongside the data.

the values of $\mathrm{cov}(c_2\{4\}, [p_{\rm T}])$ are multiplied by 4 in all the panels. As $N_{\rm ch}$ decreases in PbPb collisions, the values of $\mathrm{cov}(c_2\{2\}, [p_{\rm T}])$ change from positive to negative, reach a minimum at $N_{\rm ch} \approx 60$, and then approach zero at the lowest N_{ch} range.

The correlator with a wider η gap ($|\eta| > 1.0$) for the cumulant is shown in fig. 2. The sign change at low $N_{\rm ch}$ disappears with the larger η gap between the two subevents in both pp and pPb collisions, which is also observed in calculations using PYTHIA8. The predictions in pPb collisions at 5.02 TeV from the IP-Glasma+MUSIC+UrQMD model [14] with $0.5 < p_{\rm T} < 5$ GeV are compared with the data in fig. 2. This model includes gluon saturation in the initial state followed by hydrodynamic evolution and hadronic interactions. The characteristic sign change of the correlator predicted by this model is observed in data at the same $N_{\rm ch}$ location for $|\eta| > 0.75$, but it disappears when using $|\eta| > 1.0$, which leads to less nonflow effects. The results indicate that after removing more nonflow effects, the CGC signal is not observed in the data. More nonflow studies incorporated in the CGC model are needed to understand the origin of azimuthal anisotropy in small systems.

In all three collision systems, the correlator is negative for $n = 3$. A comparison is made with predictions from a hydrodynamic simulation of pPb collisions [19] using $p_{\rm T} > 0.5$ GeV and having an average root-mean-square (RMS) transverse radius of the initial fireball of either 0.9 or 1.5 fm. Qualitatively, the data are better described by the smaller initial fireball.

REFERENCES

[1] STAR Collaboration, *Phys. Rev. Lett.*, **95** (2005) 152301.
[2] STAR Collaboration, *Phys. Rev. C*, **80** (2009) 064912.
[3] CMS Collaboration, *JHEP*, **07** (2011) 076.
[4] ALICE Collaboration, *Phys. Rev. Lett.*, **107** (2011) 032301.
[5] ATLAS Collaboration, *Phys. Rev. C*, **86** (2012) 014907.
[6] Alver B. H., Gombeaud C., Luzum M. and Ollitrault J.-Y., *Phys. Rev. C*, **82** (2010) 034913.
[7] CMS Collaboration, *JHEP*, **09** (2010) 091.
[8] CMS Collaboration, *Phys. Rev. Lett.*, **718** (2013) 795.
[9] CMS Collaboration, *Phys. Lett. B*, **724** (2013) 213.
[10] Dusling Kevin and Venugopalan Raju, *Phys. Rev. D*, **87** (2013) 051502.
[11] Nagle J. L. and Zajc W. A., *Annu. Rev. Nucl. Part. Sci.*, **68** (2018) 211.
[12] Mazeliauskas Aleksas and Teaney Derek , *Phys. Rev. C*, **93** (2016) 024913.
[13] Schenke Björn, Shen Chun and Teaney Derek, *Phys. Rev. C*, **102** (2020) 034905.
[14] Giacalone Giuliano, Schenke Björn and Shen Chun, *Phys. Rev. Lett.*, **125** (2020) 192301.
[15] Zhang C., Behera A., Bhatta S. and Jia J., *Phys. Lett. B*, **822** (2021) 136702.
[16] Bilandzic A., Snellings R. and Voloshin S., *Phys. Rev. C*, **83** (2011) 044913.
[17] ATLAS Collaboration, *Eur. Phys. J. C*, **79** (2019) 985.
[18] CMS Collaboration, *CMS Physics Analysis Summary*, CMS-PAS-HIN-21-012, `https://cds.cern.ch/record/28059322022`.
[19] Bozek P. and Mehrabpour H., *Phys. Rev. C*, **101** (2020) 064902.